

## Supporting Information

### Alkali metal-alkaline earth metal borate crystal

### **LiBa<sub>3</sub>(OH)(B<sub>9</sub>O<sub>16</sub>)[B(OH)<sub>4</sub>] as a new deep-UV nonlinear optical material†**

Chao Wu,<sup>a</sup> Junling Song,<sup>a</sup> Longhua Li,<sup>a</sup> Mark G. Humphrey,<sup>b</sup> and Chi Zhang<sup>a\*</sup>

<sup>a</sup> China-Australia Joint Research Center for Functional Molecular Materials, School of Chemical and Material Engineering, Jiangnan University, Wuxi 214122, P. R. China

<sup>b</sup> Research School of Chemistry, Australian National University, Canberra, ACT 2601, Australia

\* Corresponding Author Email: [chizhang@jiangnan.edu.cn](mailto:chizhang@jiangnan.edu.cn)

## CONTENTS

Table S1. Selected bond distances (Å) and angles (deg) for  $\text{LiBa}_3(\text{OH})(\text{B}_9\text{O}_{16})[\text{B}(\text{OH})_4]$ .

Scheme S1.  $[\text{B}_9\text{O}_{19}(\text{OH})]^{12-}$  cluster unit constructed from  $\text{BO}_3$  and  $\text{BO}_4$  units.

Figure S1. Photograph of  $\text{LiBa}_3(\text{OH})(\text{B}_9\text{O}_{16})[\text{B}(\text{OH})_4]$ .

Figure S2. Arrangement of the  $[\text{BO}_3]^{3-}$  groups of  $\text{LiBa}_3(\text{OH})(\text{B}_9\text{O}_{16})[\text{B}(\text{OH})_4]$  along the *c*-axis.

Figure S3. Structure view of  $\text{LiBa}_3(\text{OH})(\text{B}_9\text{O}_{16})[\text{B}(\text{OH})_4]$  down the *a*-axis.

Figure S4. Coordination environments of the Ba and Li atoms in  $\text{LiBa}_3(\text{OH})(\text{B}_9\text{O}_{16})[\text{B}(\text{OH})_4]$  (a), and the 3D framework formed by the Li-O and Ba-O groups (b).

Figure S5. Experimental and simulated powder X-ray diffraction patterns of  $\text{LiBa}_3(\text{OH})(\text{B}_9\text{O}_{16})[\text{B}(\text{OH})_4]$ .

Figure S6. IR spectrum of  $\text{LiBa}_3(\text{OH})(\text{B}_9\text{O}_{16})[\text{B}(\text{OH})_4]$ .

Figure S7. UV-Vis-NIR diffuse reflectance absorption spectra of  $\text{LiBa}_3(\text{OH})(\text{B}_9\text{O}_{16})[\text{B}(\text{OH})_4]$ .

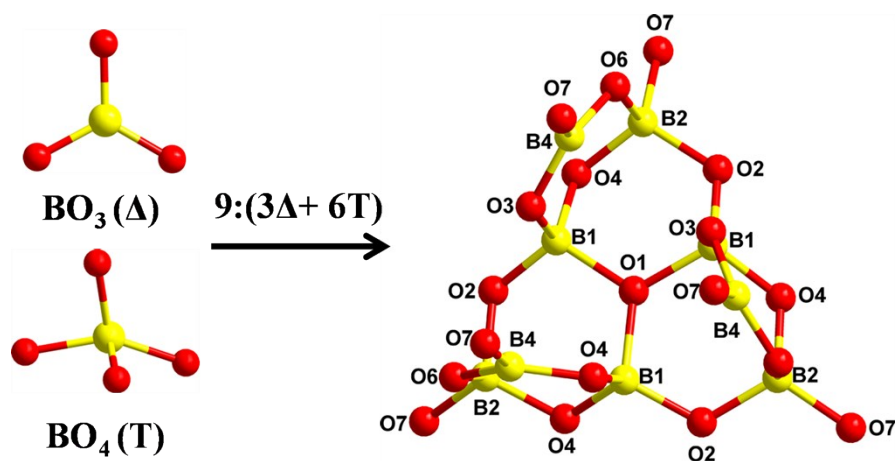
Figure S8. Band structure of  $\text{LiBa}_3(\text{OH})(\text{B}_9\text{O}_{16})[\text{B}(\text{OH})_4]$ .

Figure S9. Calculated refractive indexes of  $\text{LiBa}_3(\text{OH})(\text{B}_9\text{O}_{16})[\text{B}(\text{OH})_4]$ .

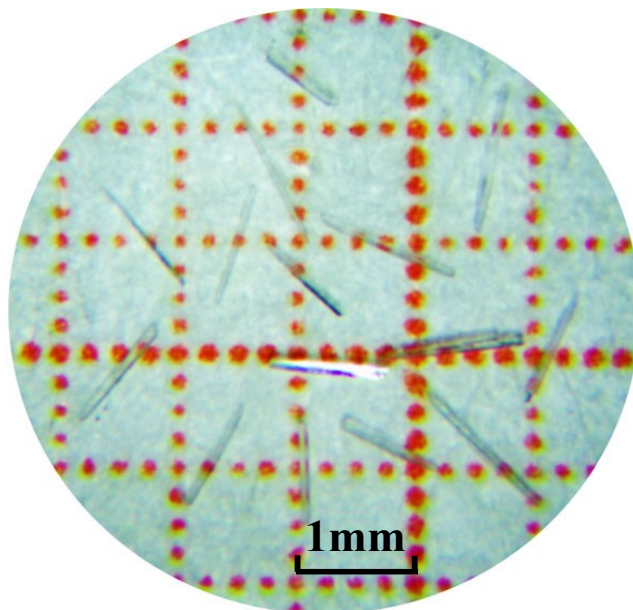
**Table S1.** Selected bond distances (Å) and angles (deg) for LiBa<sub>3</sub>(OH)(B<sub>9</sub>O<sub>16</sub>)[B(OH)<sub>4</sub>]<sup>a</sup>.

B(1)-O(4)	1.432(7)	B(1)-O(2)	1.434(7)
B(1)-O(3)	1.511(7)	B(1)-O(1)	1.519(6)
B(2)-O(4)#1	1.448(7)	B(2)-O(2)	1.466(7)
B(2)-O(7)	1.474(7)	B(2)-O(6)	1.506(7)
B(3)-O(8)#2	1.377(8)	B(3)-O(8)	1.377(8)
B(3)-O(8)#3	1.377(8)	B(3)-O(9)	1.528(15)
B(4)-O(7)#4	1.367(7)	B(4)-O(3)	1.376(7)
B(4)-O(6)#5	1.389(7)		
Ba(1)-O(2)	2.747(4)	Ba(1)-O(2) #7	2.871(3)
Ba(1)-O(3)	2.925(4)	Ba(1)-O(4) #7	2.677(4)
Ba(1)-O(5)	2.7097(11)	Ba(1)-O(6)	3.065(4)
Ba(1)-O(6) #8	2.780(4)	Ba(1)-O(7) #8	3.032(4)
Ba(1)-O(8)	3.103(11)	Ba(1)-O(8) #7	2.993(10)
Ba(1)-O(9)#7	2.852(14)		
Li(1)-O(3) #9	2.595(18)	Li(1)-O(3) #6	2.595(18)
Li(1)-O(3) #10	2.595(18)	Li(1)-O(5)	1.81(2)
Li(1)-O(7)	2.239(4)	Li(1)-O(7) #8	2.239(4)
Li(1)-O(7) #11	2.239(4)		
O(4)-B(1)-O(2)	109.9(4)	O(4)-B(1)-O(3)	109.8(4)
O(2)-B(1)-O(3)	112.0(4)	O(4)-B(1)-O(1)	108.1(4)
O(2)-B(1)-O(1)	110.0(4)	O(3)-B(1)-O(1)	106.9(4)
O(4) #1-B(2)-O(2)	111.7(4)	O(4) #1-B(2)-O(7)	111.4(4)
O(2)-B(2)-O(7)	111.2(4)	O(4) #1-B(2)-O(6)	107.9(4)
O(2)-B(2)-O(6)	107.8(4)	O(7)-B(2)-O(6)	106.5(4)
O(8)-B(3)-O(8) #2	119.57(15)	O(8)-B(3)-O(8) #3	119.57(15)
O(8) #2-B(3)-O(8) #3	119.57(15)	O(8) #2-B(3)-O(9)	118.5(9)
O(8) #3-B(3)-O(9)	98.7(9)	O(9)-B(3)-O(8)	98.7(9)
O(7) #4-B(4)-O(3)	116.9(5)	O(7) #4-B(4)-O(6) #5	122.0(5)
O(3)-B(4)-O(6) #5	121.1(5)		

<sup>a</sup> Symmetry codes: #1 - y+1, x-y+1, z; #2 -y, x-y, z; #3 -x+y, -x, z;  
 #4 x-y, -y+1, z-1/2; #5 -x+y, -x+1, z; #6 -x+1, -x+y, z+1/2;  
 #7 x, y, z-1/2; #8 -y+1, x-y, z; #9 x, y, z+1/2;  
 #10 x-y+1, -y+1, z+1/2; #11 -x+y+1, -x+1, z.



**Scheme S1.**  $[\text{B}_9\text{O}_{19}(\text{OH})]^{12-}$  cluster unit constructed from  $\text{BO}_3$  and  $\text{BO}_4$  units.



(a)

**Figure S1.** Photograph of  $\text{LiBa}_3(\text{OH})(\text{B}_9\text{O}_{16})[\text{B}(\text{OH})_4]$ .

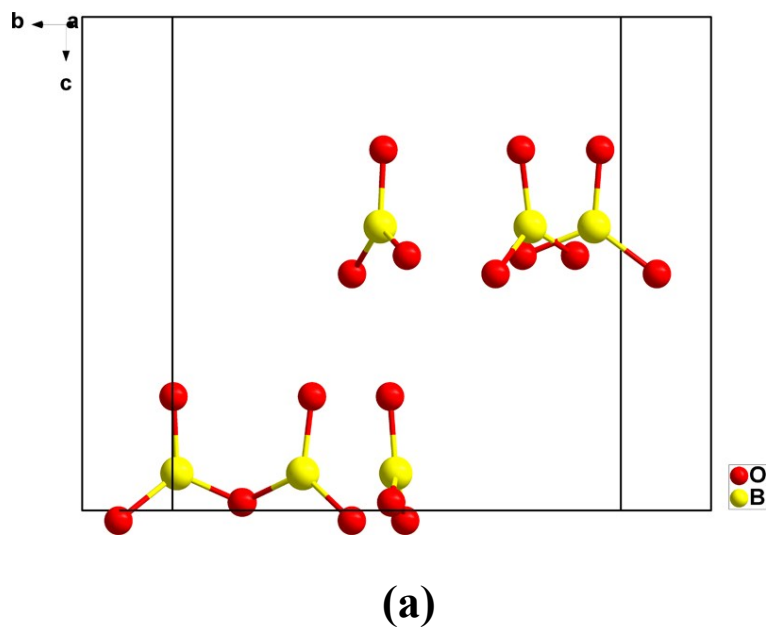


**Figure S2.** Arrangement of  $[\text{BO}_3]^{3-}$  groups of  $\text{LiBa}_3(\text{OH})(\text{B}_9\text{O}_{16})[\text{B}(\text{OH})_4]$  along the  $c$ -axis.

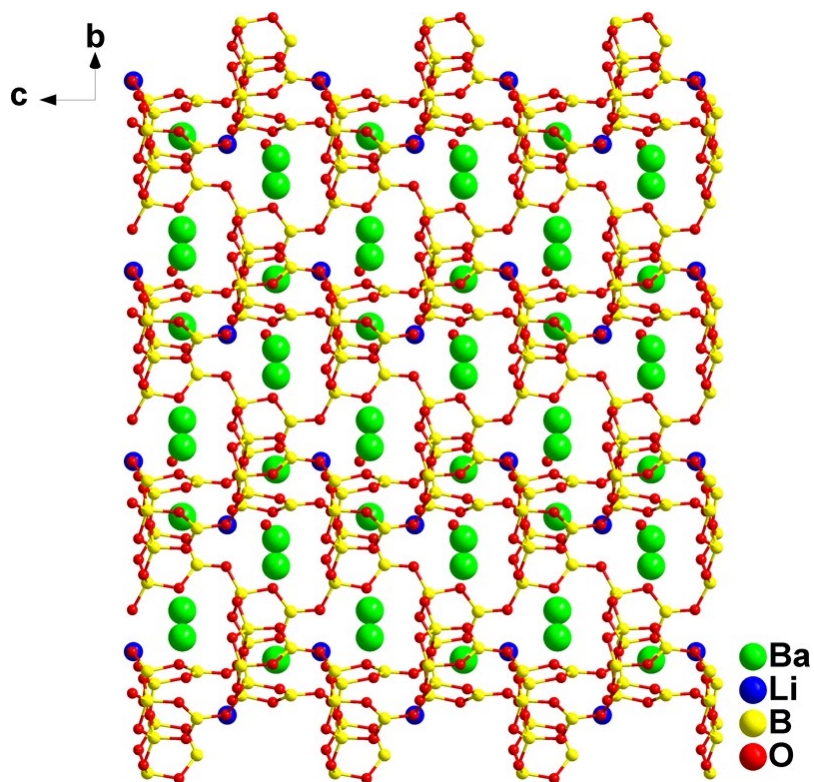


**Figure S3.** Structure view of  $\text{LiBa}_3(\text{OH})(\text{B}_9\text{O}_{16})[\text{B}(\text{OH})_4]$  down the  $a$ -axis.

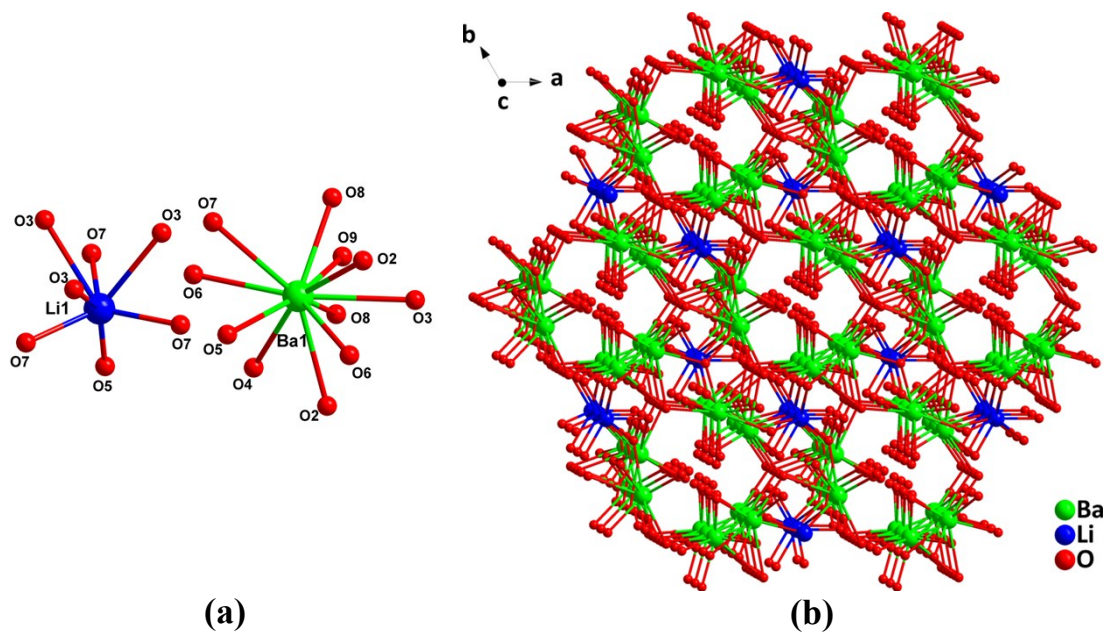


**Figure S4.** Coordination environments of the Ba and Li atoms in  $\text{LiBa}_3(\text{OH})(\text{B}_9\text{O}_{16})[\text{B}(\text{OH})_4]$  (a), and the 3D framework formed by the Li-O and Ba-O groups (b). Hydrogen atoms have been omitted for clarity.



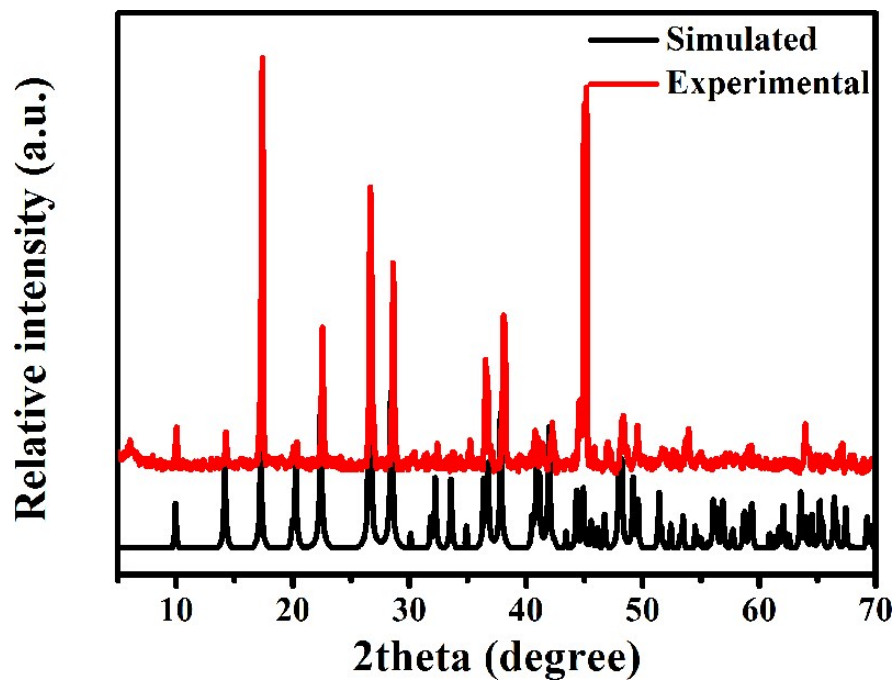


**Figure S5.** Experimental and simulated powder X-ray diffraction patterns of  $\text{LiBa}_3(\text{OH})(\text{B}_9\text{O}_{16})[\text{B}(\text{OH})_4]$ .

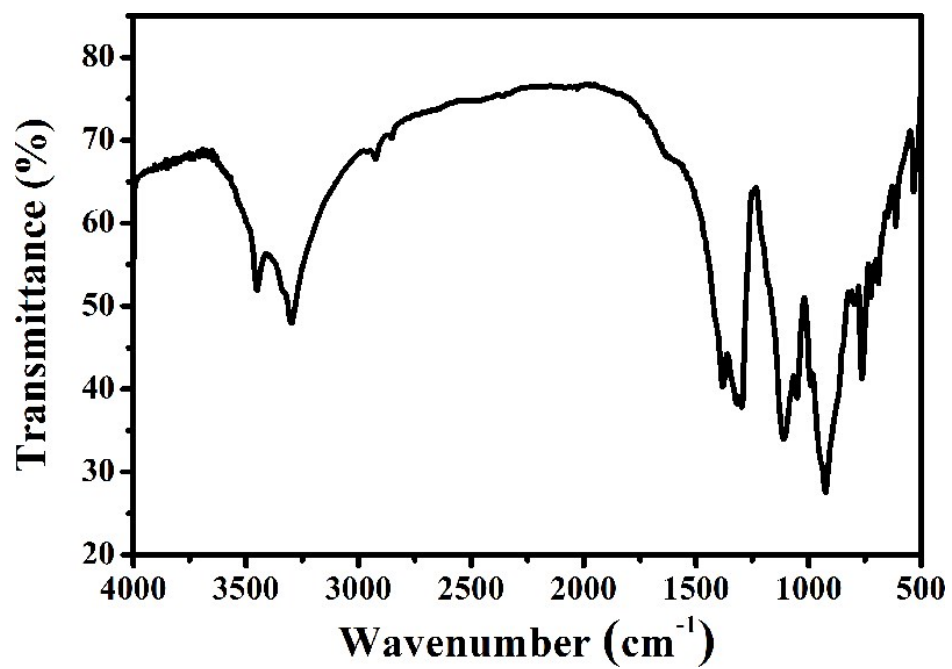
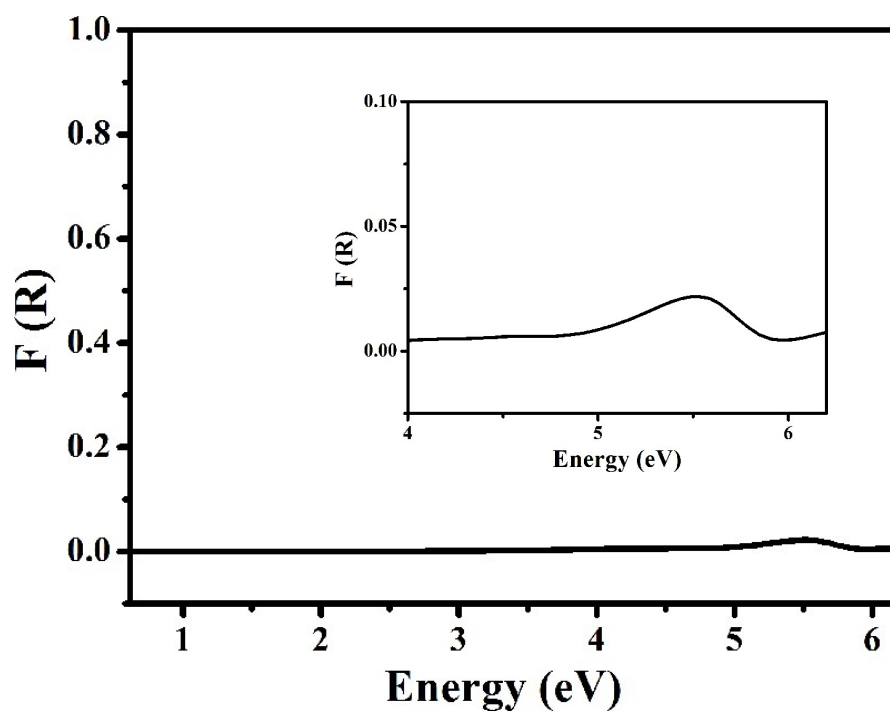
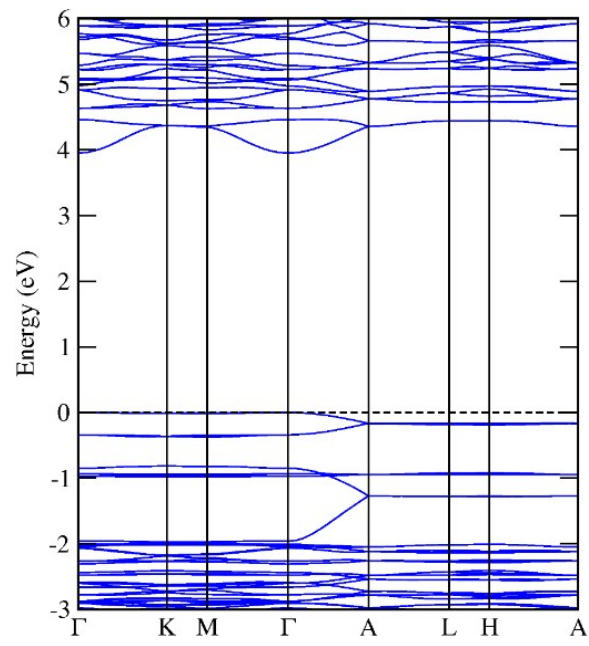


Figure S6. IR spectrum of  $\text{LiBa}_3(\text{OH})(\text{B}_9\text{O}_{16})[\text{B}(\text{OH})_4]$ .



**Figure S7.** UV-Vis-NIR diffuse reflectance absorption spectra of  $\text{LiBa}_3(\text{OH})(\text{B}_9\text{O}_{16})[\text{B}(\text{OH})_4]$ .



**Figure S8.** Band structure of  $\text{LiBa}_3(\text{OH})(\text{B}_9\text{O}_{16})[\text{B}(\text{OH})_4]$ .

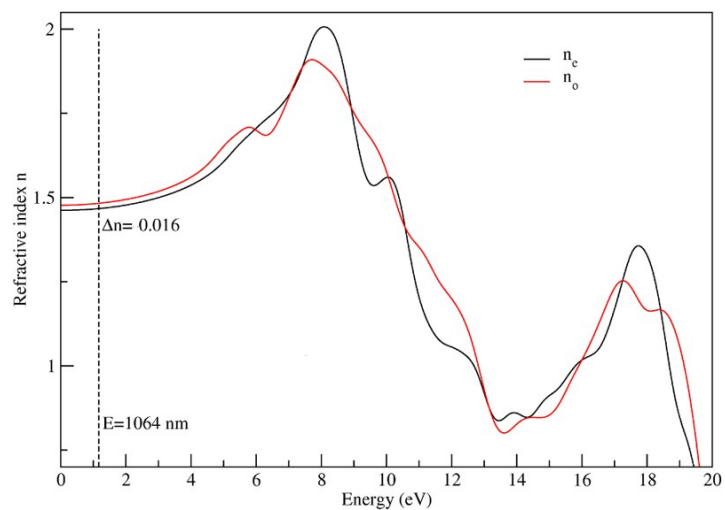


**Figure S9.** Calculated refractive indexes of  $\text{LiBa}_3(\text{OH})(\text{B}_9\text{O}_{16})[\text{B}(\text{OH})_4]$ .